

An Overconstrained Robotic Leg with Coaxial Quasi-direct Drives for Omni-directional Ground Mobility*

Shihao Feng, Yuping Gu, Weijie Guo, Yuqin Guo, Fang Wan, Jia Pan and Chaoyang Song*

Abstract—Planar mechanisms dominate modern designs of legged robots with remote actuator placement for robust agility in ground mobility. This paper presents the novel design of an overconstrained robotic leg driven by two coaxially arranged quasi-direct actuators, capable of omni-directional ground locomotion. We investigated the design, modeling, and optimization of a robotic leg module based on the Bennett linkage, which is an overconstrained 4R linkage often exhibited with three-dimensional motion and unparalleled joint axes. We further explored the reconfigurable design using this Bennett leg module, resulting in a large class of overconstrained robots as a potential direction for novel designs of legged robots.

Index Terms—Overconstrained Robots, Bennett linkage, Legged Robots, Reconfigurable Design

I. INTRODUCTION

Modern designs of robotic legs require balanced robustness for agile locomotion. When dexterous manipulation is a higher priority, a serial arrangement of actuation and robot structure is usually chosen with four to seven degree-of-freedoms (DoFs). However, when robust agility becomes a primary concern, it is common to either choose parallel mechanisms with redundant constraints or high-performing actuators at an expensive cost. Many recent legged robots are designed with no more than three DoFs per leg using various planar mechanisms with a remote placement of actuators for enhanced robustness in agile locomotion.

It is a common practice in engineering design to reduce the total number of parts to enhance the system's robustness at a reduced cost. For example, legged robots such as RHex [1], isprawl [2], and XRL [3] are designed with only one DoF per robot or per leg with continuous and reversible rotation at an adjustable speed, achieving a minimum design with reliable robustness at a low-cost. To a certain extent, such robots may be considered with a closer relationship to wheeled robots than legged robots in modeling and control.

*This work was supported by Southern University of Science and Technology and AncoraSpring Inc.

S. Feng, Y. Guo, W. Guo are with the Department of Mechanical and Energy Engineering, Southern University of Science and Technology, Shenzhen, Guangdong 518055, China. (e-mail: {12032726, 11510615, 12032421}@mail.sustech.edu.cn, wuj@sustech.edu.cn)

Y. Gu is with the Southern University of Science and Technology, Shenzhen, Guangdong 518055, China, and also with the University of Hong Kong, Pokfulam, Hong Kong (e-mail: u3007411@connect.hku.hk)

F. Wan is a Visiting Scholar with the Department of Mechanical and Energy Engineering, Southern University of Science and Technology, Shenzhen, Guangdong 518055, China. (e-mail: sophie.fwan@hotmail.com)

J. Pan is with the Department of Computer Science, University of Hong Kong, Pokfulam, Hong Kong (email: jpan@cs.hku.hk).

C. Song is the corresponding author with the Department of Mechanical and Energy Engineering, Southern University of Science and Technology, Shenzhen, Guangdong 518055, China. (email: songcy@ieee.org)

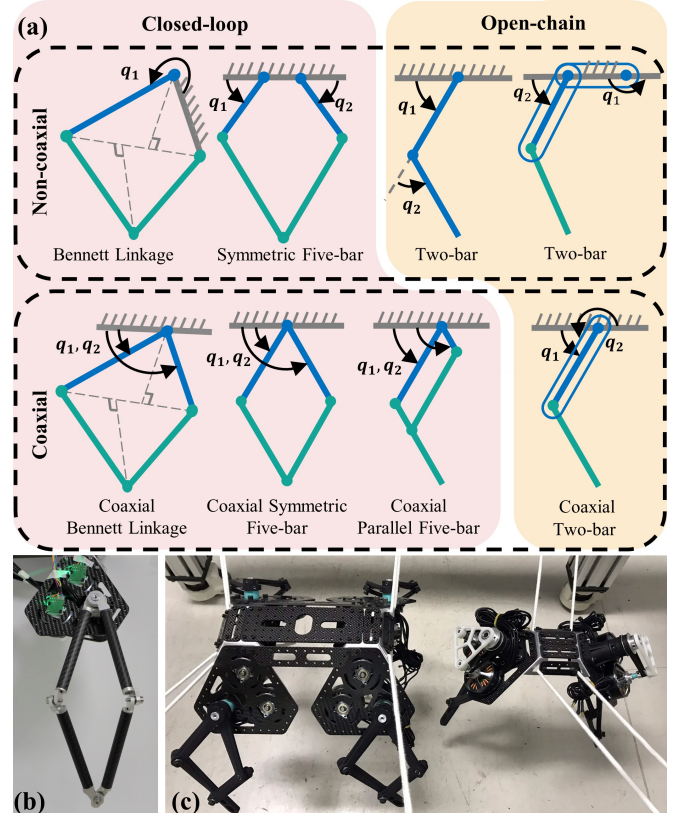


Fig. 1: An overview of leg mechanisms and the proposed robotic Bennett leg. (a) An overview of mechanisms for legged robots including close-loop [4], [5], [6], [7] and open-chain [8], [9], [10], [11]. The driving links in blue and driven links in green. (b) The robotic Bennett leg with quasi-direct drives proposed in this paper. (c) Preliminary prototypes of overconstrained quadruped and bipedal robot.

Robustness improvement and weight reduction within a compact form factor is another design consideration for multi-legged robots, where an engineering strategy with coaxially arranged actuators become a popular design with two or three DOFs in each leg. As illustrated in Fig. 1(a), robots such as Minitaur [5], Stanford Doggo [6], and MIT Cheetah [7] adopted a two-DoF leg design to improve stability and versatility while maintaining lightweight and reliability in unstructured locomotion. Due to the kinematic constraints in the sagittal plane, it is difficult for a robot with two-DoF planar legs to change the direction of movement, which is usually achieved through differential velocities with a relatively large turning radius, limiting its agility in the narrow environment. Inspired by the mammalian-

like locomotion, Cheetah-cub-S utilizes an actuated lateral bending spine to improve the steering ability, but still unable to feature some agile maneuvers such as turning on the spot [12].

Robots with advanced locomotion are usually designed with three DoFs per leg, where an extra actuator is usually attached to the base of the two-DoF legs for high-speed maneuvering [10], agile walking [13], or rugged terrain adaptation [14]. And robotic leg such as GOAT [15] and 3-UPR leg [16] use a spatial tri-link mechanism with three actuators evenly arranged to obtain three-dimensional agility. However, with the introduction of an extra actuator in each leg, the total number of actuators will increase by 50%, posing challenges to manage the robot's total weight, the system's cost, the energy consumption, and robustness. Quasi-direct drive (QDD) becomes a preferred choice for such robots to provide agile reaction within a compact form factor, and many high-performance robots are built with custom actuators at an expensive cost [11], [17]. We believe that the mechanical advantages of mechanism design in power transmission and motion generation still present novel designs for fundamental research and development.

In this paper, we propose a novel design of leg modules for omni-directional locomotion by using an overconstrained Bennett linkage actuated by two coaxially arranged quasi-direct drives, as shown in Fig. 1, to achieve a coupled, spatial trajectory at the tip of the leg. The Bennett linkage is among a class of linkages with specialized geometry, which are considered overconstrained using the classical Kutzbach's criterion, yet still movable with three-dimensional (3D) trajectories. The Bennett linkage can be considered a generalization of the planar four-bar linkage with unparallelized joint axes or non-zero twist angles. Contributions of this paper are listed as follows:

- Kinematics and parameter optimization of the coaxial Bennett linkage for legged robots;
- Design and development of a two-DoF overconstrained Bennett leg towards omni-directional ground mobility;
- Experimental validation of the coupled three-dimensional motion of the overconstrained Bennett leg and simulation of an overconstrained quadruped;
- Preliminary guidelines of reconfigurable design for a new class of overconstrained robots.

The rest of this paper is organized as the following. Section II presents the theoretical development of the Bennett linkage as a robotic leg. Section III describes the engineering design of the robotic Bennett leg module with quasi-direct drives. Experiment results are presented in section IV, which is followed by a discussion of the results in section V. Final remarks are enclosed in section VI, which ends this paper.

II. THEORETICAL DEVELOPMENT TOWARDS A ROBOTIC BENNETT LEG

A. Modeling the Bennett Linkage with Coaxial Actuation

The Bennett linkage [18] is geometrically defined by the following conditions, with a_{ij} as the length of link ij , α_{ij}

as the twist of link ij , and R_i as the offset of joint i .

$$\begin{aligned} a_{12} &= a_{34} = a, a_{23} = a_{41} = b, \\ \alpha_{12} &= \alpha_{34} = \alpha, \alpha_{23} = \alpha_{41} = \beta, \\ \frac{\sin \alpha}{a} &= \frac{\sin \beta}{b}, \\ R_i &= 0 \quad (i = 1, 2, 3, 4). \end{aligned} \tag{1}$$

The explicit closure equations of the Bennett linkage are as follows [19], with θ_i as the revolute variable of joint i . It is obvious that the Bennett linkage becomes a planar four-bar linkage when the joint axes are parallel.

$$\begin{aligned} \theta_1 + \theta_3 &= 2\pi, \theta_2 + \theta_4 = 2\pi, \\ \tan \frac{\theta_1}{2} \tan \frac{\theta_2}{2} &= \frac{\sin \frac{\beta+\alpha}{2}}{\sin \frac{\beta-\alpha}{2}}. \end{aligned} \tag{2}$$

Typical analysis of mechanism kinematics assumes a base link fixed to the ground with a reference frame attached. For example, many modern robotic legs adopt a five-bar linkage with a base link fixed to the robot body, which has two DoFs. Two actuators can be attached to the two joint axes of the based link to control the leg motion fully. To achieve a compact form factor, it is common to reduce the length of the five-bar linkage's base link to zero, resulting in a coaxial arrangement of the two actuators. From another perspective, one could view this approach as a rotating base link method by attaching the referencing frame to a fixed joint axis of a planar four-bar linkage, then adding two actuators to the two adjacent links.

We can apply the same approach with coaxially arranged actuators for the Bennett linkage to make it a leg mechanism, as shown in Fig. 1(b). By examine the closure equations in Eq. (2), it is evident that the resultant leg will behave with a coupled, spatial trajectory in 3D space driven by only two actuators, which is different from the 2D trajectories with planar mechanisms as robotic legs. It should be noted that one can also conveniently replace the Bennett linkage with other overconstrained linkages to achieve a novel class of leg designs with coupled spatial motion.

To facilitate the kinematic analysis from overconstrained linkages to robotic legs, one can view the coaxially-driven Bennett linkage equivalent to a serial two-DoF linkage with coupled motion, as shown in Fig. 2. In Fig. 2(a), a and b are the lengths of links 12 and 23 respectively, α and β are the twist angle of links 12 and 23, respectively. σ is the angle of abduction which is generally actuated by hip joint in three-DoF leg designs. In our design, σ is a constant and chosen for adjusting the ground contact posture of tip.

Therefore, we can write the homogeneous transformation matrix of the two-bar linkage from the base frame $\{w\}$ to the foot frame $\{3\}$ using the product of exponentials formula as

$${}^w T = e^{[\mathcal{S}_1]\varphi_1} e^{[\mathcal{S}_2]\varphi_2} M, \tag{3}$$

where \mathcal{S}_1 and \mathcal{S}_2 are the screw axes, M is the position and orientation of frame $\{3\}$ when all joint angles are zero. When

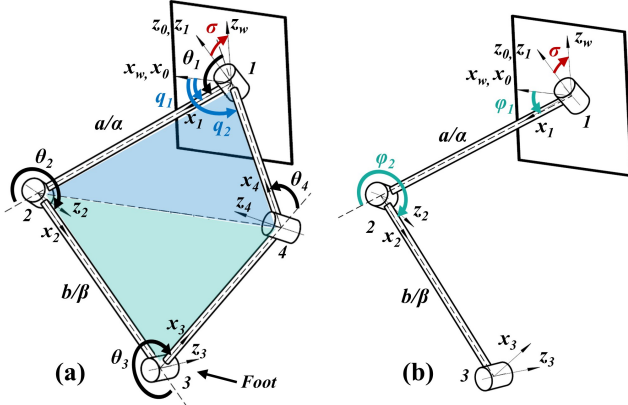


Fig. 2: The kinematic diagram of the proposed overconstrained Bennett leg. (a) A coaxial Bennett linkage. Red arrow represents the pitch angle of the hip joint σ . Blue arrows describe the actuator angles (q_1, q_2). (b) A serial two-bar linkage. Green arrows describe the joint angles (φ_1, φ_2).

expressed in frame $\{w\}$, we can write

$$\mathcal{S}_1 = \begin{bmatrix} 0 \\ 0 \\ 0 \\ 0 \\ s\sigma \\ c\sigma \end{bmatrix}, \quad \mathcal{S}_2 = \begin{bmatrix} 0 \\ -ac(\alpha - \sigma) \\ -as(\alpha - \sigma) \\ 0 \\ -s(\alpha - \sigma) \\ c(\alpha - \sigma) \end{bmatrix}, \quad (4)$$

$$M = \begin{bmatrix} 1 & 0 & 0 & a+b \\ 0 & c(\alpha + \beta - \sigma) & -s(\alpha + \beta - \sigma) & 0 \\ 0 & s(\alpha + \beta - \sigma) & c(\alpha + \beta - \sigma) & 0 \\ 0 & 0 & 0 & 1 \end{bmatrix}, \quad (5)$$

where $s\sigma$ and $c\sigma$ denote $\sin \sigma$ and $\cos \sigma$, respectively.

From Eq. (2), the transformation between the actuator angles (q_1, q_2) and the joint angles of the two-bar linkage model (φ_1, φ_2) are as follow,

$$\varphi_1 = q_1, \quad (6)$$

$$\varphi_2 = \arctan(K \tan(\frac{q_2 - q_1}{2})), \quad (7)$$

where $K = \sin(\frac{\beta+\alpha}{2})/\sin(\frac{\beta-\alpha}{2})$ is a constant based on Eq. (2). And the differentiation of Eqs. (6) and (7) can be expressed as

$$\dot{\varphi} = \begin{bmatrix} 1 & 0 \\ -H & H \end{bmatrix} \dot{q}, \quad (8)$$

where $H = [K \sec^2(\frac{q_2 - q_1}{2})]/[1 + K^2 \tan^2(\frac{q_2 - q_1}{2})]$. Therefore, the jacobian $J_s(q) \in \mathbb{R}^{6 \times 2}$ mapping between actuator rate vector $\dot{q} \in \mathbb{R}^2$ and the spatial twist \mathcal{V}_s can be computed as

$$\mathcal{V}_s = J_s(q)\dot{q} = \begin{bmatrix} J_{s1} - H J_{s2} & H J_{s2} \end{bmatrix} \begin{bmatrix} \dot{q}_1 \\ \dot{q}_2 \end{bmatrix}, \quad (9)$$

where $J_{s1} = \mathcal{S}_1$, $J_{s2} = [Ad_{e[\mathcal{S}_1]\varphi_1}] \mathcal{S}_2$. $[Ad_T]$ represents the adjoint matrix based on the homogeneous transformation matrix.

Similar to the two-bar serial mechanism, the Bennett linkage also has boundary singularities when the axis of

links are colinear ($q_2 - q_1 = 0/\pi$). However, it is hard for the overconstrained linkages to achieve full-cycle rotation like a planar mechanism. Thus, singularities can be avoided practically through the mechanical design of linkages, see Fig. 6(a).

B. Design Parameter Selection and Optimization

This section is devoted to the parameter selection for the design of a robotic Bennett leg for omni-directional locomotion. By considering the workspace and force transmission, the following design parameters are considered, including link lengths a and b and twist angles α and β in Eq. (1), and pitch angle of the hip joint σ in Eqs. (4) and (5).

Due to the Bennett leg's coupled spatial motion, we investigated a suitable selection of design parameters for omni-directional locomotion. We set the total length of the each leg as $a + b = 0.3m$, with $a \in [0.15, 0.295]$ and $\alpha \in (90, 180]$ to narrow down the range of valid selection as a leg mechanism. The geometric parameter β is obtained by solving the constraint equation of Eq. (1). As shown in Fig. 3(a), the result indicates that when a and b are fixed, the smaller the value of α , the larger the workspace. It also reveals that when α is fixed and $a = b$, the workspace is the largest. In addition, the workspace of the Bennett linkage is symmetrical about the frontal plane when $a = b$. Symmetry both of configuration and workspace is prioritized for an omni-directional walking robot. Therefore, the four links of the coaxial Bennett linkage are designed to have the same length of 0.15m, and the variables of the design parameter are narrowed down to $p = [\alpha, \sigma]$.

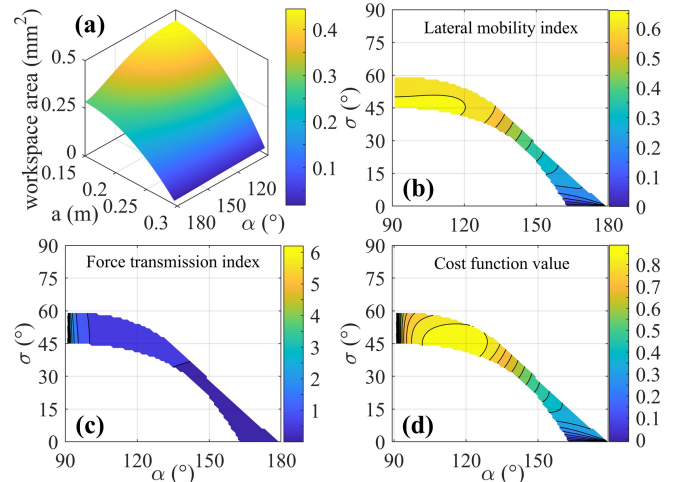


Fig. 3: Results of the parameter optimization. (a) Workspace in the parameter space. (b) Lateral mobility index. (c) Force transmission index. (d) Comprehensive objective function value.

A distinctive feature of the proposed Bennett leg is lateral walking or turning on the spot, besides common requirement on forwarding locomotion. The sufficient condition for lateral locomotion requires the planes' reachable trajectory parallel to the YZ -plane to be non-monotonic. A stance phase trajectory can be described by the stride length and vertical amplitude, as described in Fig. 4. An index for lateral

mobility evaluation is defined as the utilization of workspace for lateral walking minus the relative change of body height.

$$C_{lm}(p) = w_y \frac{y_{sl}}{y_{max}} - w_z \frac{z_{da}}{z_{max}}, \quad (10)$$

where y_{sl} and z_{da} are the maximum stride length and the maximum down amplitude, y_{max} and z_{max} are the maximum range of motion in Y -direction and Z -direction respectively. w_y , w_z are the weights for the Y -direction and Z -direction terms, both set as 1 in our design.

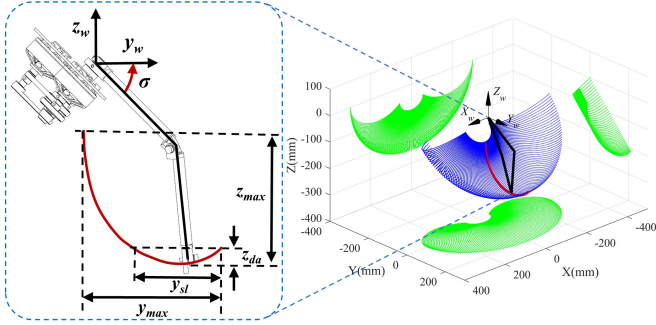


Fig. 4: The evaluation indexes description and the workspace of the coaxial Bennett linkage ($\alpha = \frac{2\pi}{3}$, $\sigma = \frac{\pi}{4}$). Red line is the reachable motion trajectory on YZ -plane.

We also take the force transmission capability of the robotic Bennett leg into account, which is crucial to decrease the required motor torque. The force transmission index is defined as the maximum output torque for a given walking trajectory under the ground reaction force (GRF) as below.

$$C_{ft}(p) = \max \{ \|\tau_1(i)\|, \|\tau_2(i)\| \mid i = 1, 2, \dots, N \}. \quad (11)$$

The applied actuator torques is estimated by using the leg Jacobian to convert the GRF,

$$\begin{bmatrix} \tau_1(i) \\ \tau_2(i) \end{bmatrix} = J_s^T(q_i)f, \quad (12)$$

where $\tau_1(i)$ and $\tau_2(i)$ are the required actuator torques at the i th state of stance phase. We assume an X -direction trajectory with a stride length of 0.1m. N is the number of sampling points of a walking trajectory. f is the GRF which is assumed as vertical with a size of 49N (equivalent to a 5kg payload).

Finally, the optimization problem is formulated as

$$\max \quad w_{lm} C_{lm}(p) - w_{ft} \frac{C_{ft}(p)}{C_{ft}(p)_{max}},$$

$$\begin{aligned} & \alpha + \beta = 2\pi, \\ & a \leq y_{sl}, \\ \text{s.t. } & 0 \leq z_{da} < 0.3a, \\ & \pi/2 < \alpha < \pi, \\ & 0 \leq \sigma < \pi/2, \\ & 0 \leq q_2 - q_1 \leq \pi \end{aligned} \quad (13)$$

where w_{lm} and w_{ft} are the weights for the lateral mobility index and force transmission index terms, which are set as 1

in our design. And the equality constraint is derived by Eq. (1).

As shown in Eq. (13), the parameter set for optimization only involves two variables. Therefore, finding the optimal solution using an exhaustive method computes the cost function's value for all parameter sets. All parameter sets at steps of one degree within the range of the valid parameters are generated. Then, the values of the lateral mobility index and force transmission index are calculated, and the result is illustrated in Figs. 3(b) and (c). The cost function is calculated based on the two standardized evaluation metrics, and the result is in Fig. 3(d). The best design is obtained around the parameter set [116, 44] with a cost of 0.889. For practical fabrication, a nearby parameter set [120, 45] with the cost of 0.885 is selected, with the workspace presented in Fig. 4(b).

C. Projection-based Trajectory Generation

The foot trajectories implemented on the robotic Bennett leg are designed in the projected planes because of its coupled three-dimensional workspace. Fig. 5 shows the foot trajectories used for the quadruped in forward walking, lateral walking, and turning. The trajectories used on the robotic Bennett leg are a projected straight line and a projected cycloid for the stance and swing phases under the constraints of stride length, ground clearance, and velocity smoothness. The open-loop trajectory has successfully applied to the previous dynamic quadruped [20]. Although the open-loop trajectory will introduce discontinuities in acceleration, the belt drive design in quasi-direct actuator (see Section III-B) can effectively alleviate its impact. For fast calculation, the actuator angles are solved by the method of velocity differentiation rather than inverse kinematics.

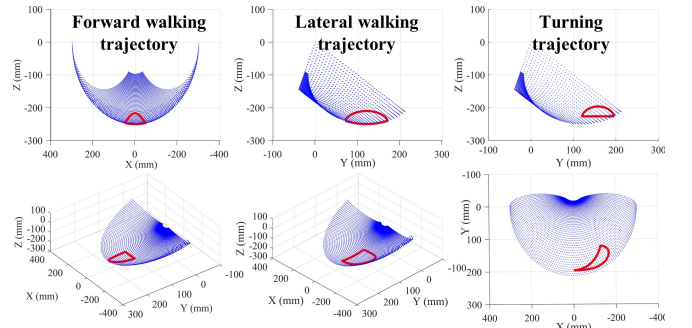


Fig. 5: Three walking trajectories in different directions, including forward walking (left), lateral walking (middle), and turning (right).

III. ENGINEERING DESIGN WITH QUASI-DIRECT DRIVES

This section is devoted to the engineering design of the robotic Bennett leg as a modular system. We begin with details of the low-inertia leg design with carbon tubes, followed with actuation using coaxially arranged quasi-direct drives with BLDC motors and belt transmission for dynamic locomotion with proprioception. The resultant robotic Bennett leg module weighs 850g.

A. Mechanical Design of a Bennett Leg

Robots built with closed-loop linkages often suffer from a limited relative rotation range, where the adjacent links interfere when close to a colinear configuration. Therefore, an alternative form design of the Bennett linkage is adopted, where the kinematic relationship is fully preserved, but a different mechanical structure is used with redundant offsets. Shown in Fig. 6(c) is the resultant design, which is capable of achieving a fully colinear configuration without collision. Fig. 6(b) shows the three parts of each link, including two aluminum hinges with offsets, machined using 7075 aluminum. An off-the-shelf carbon fiber tube with 1.5mm thickness is used to ensure sufficient strength while keeping a lightweight assembly. The two sides of the carbon fiber tube are respectively bonded with the aluminum hinge by epoxy adhesive (3M DP460). The length of the assembled links depends on the size of the carbon fiber tube. Using this design, one can easily modify the link's length and twist to build robots using different overconstrained linkages with an increased range of motion while avoiding an unnecessary collision. In addition, the planar four-bar linkages can also be constructed by using these links with a parallel twist.

As shown in Figs. 6(c) and (d), the resultant linkage design weigh only 141g with the inertia of 0.0049kgm^2 in a straight configuration, and the range of the angle of two actuated links is $0 - 110^\circ$. Moreover, four legs' total mass is 11.3% of a fully assembled quadruped with an estimated total weight of 5kg. The finite element analysis was performed to verify the strength of the Bennett leg. The results in Fig. 6(e) indicate that the maximum stress up to 187.84Mpa at the aluminum hinge, which was far less than the yield strength of 7075 aluminum with 503Mpa. Further optimization is possible with this engineering design, which can be determined when the full-sized robot is built.

B. Coaxial Actuation with Quasi-Direct Drives

The parallel arrangement of actuators delivers GRF with a uniform distribution, allowing sufficient force to be generated at the foot with a lower gear ratio, resulting in high force transparency [22]. As a conservative compromise, the proposed robotic Bennett leg was implemented using two quasi-direct drives (QDDs) with coaxial outputs. Fig. 7 shows a modular design adapted from the open-sourced Stanford Doggo, a quadruped with planar five-bar linkage leg [6].

A triangular plate from carbon fiber is designed with two corners fixed with two brushless motors (T-Motor MN5212 KV340), each attached with a magnetic rotary encoder (ams AS5047D). The plate's third corner is fixed with two coaxially assembled shafts through a 3.75 : 1 timing belt transmission each. Two links are attached to the inner and outer shafts (6061 aluminum) at the same time to deliver a wide range of leg rotation while providing sufficient protection to the actuators from falling. As a result, a compact form factor and lightweight design are achieved for the robotic Bennett leg module with dual coaxially arranged QDDs. We also added a series of holes along the edges of the carbon plate for reconfigurable assembly. It is worth noting that this

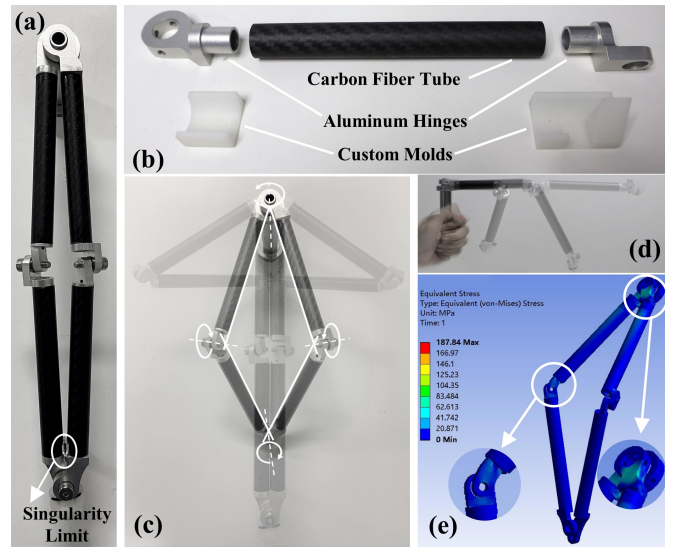


Fig. 6: The proposed coaxial Bennett linkage. (a) The prototype of the coaxial Bennett linkage whose singularities are avoided. (b) Components required for a link fabrication. (c) Different configurations of the coaxial Bennett linkage in the motion range of $0 - 110^\circ$ in top view, white lines represent the theoretical axis. (d) Different configurations of the coaxial Bennett linkage in the motion range of $0 - 110^\circ$ in side view. (e) The equivalent stress under the vertical GRF of 127.4N (a payload equivalent to 2.6 times of the weight of a quadruped robot [21]) in a stance configuration.

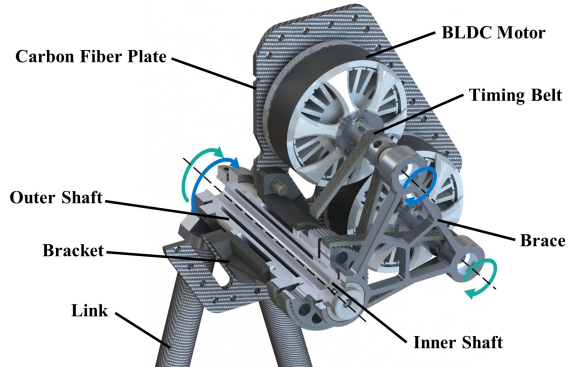


Fig. 7: The assembly of the coaxial QDD actuator module. Blue and green arrows represent one belt drive from motor shaft to active link of linkage.

linkage design with coaxial outputs is also applicable to other overconstrained linkages with $5R$ or $6R$ configurations [23].

All electronics are fixed within a removable box to facilitate a modular design: the microcontroller, onboard PC, and the DC-DC converter on the upper layer; four (or more, if necessary) dual-channel motor controllers (ODrive V3.6) on the middle layer; and another two Li-Po batteries with a nominal voltage of 24V on the lower layer, keeping a low center of gravity (CoG).

IV. EXPERIMENT AND RESULTS

We conducted experimental verification of the proposed leg design with Bennett linkage through simulations of forward walking, lateral walking, and turning on-the-spot.

We also tested the spatial trajectories of these gait patterns using the single-leg prototype.

A. Walking Simulations of an Overconstrained Quadruped

Based on the leg module presented in Fig. 7, we assembled a simplified quadruped with an estimated weight of 5kg in CAD, measured at 0.437m in length, 0.256m in width, and 0.133m in height. All simulations were run in *CoppeliaSim* using the Newton physics engine. The friction coefficient is set high to prevent the robot from slipping. For verification of the omni-directional locomotion, three simulation experiments were conducted, including walk forward and sideways and turning on the spot. Furthermore, these simulations were performed in a trotting gait using position control.

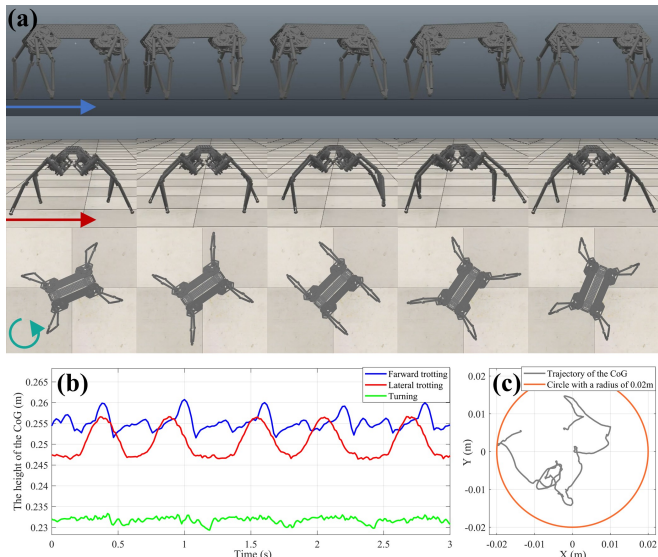


Fig. 8: Simulation results. (a) The sequence of images depicting the forward trotting, lateral trotting, and turning on the spot. (b) The height of the CoG of the robot during movement. (c) The trajectory of CoG during turning on the spot.

Shown in Fig. 8(a) are the image sequence of the three gait patterns. The result shows that the quadruped with the overconstrained Bennett leg is capable of walking forward. Even with only two actuators per leg, the quadruped can walk sideways and gait behavior similar to the crabs. Furthermore, simulation results show that the quadruped can even make turns on the spot, achieving omni-directional capability without extra advanced control or extra actuation. Fig.8(b) shows the recorded height of CoG shows a certain level of fluctuation during forward and lateral trotting, measured at 9.2mm and 10.3mm maximum in the vertical direction, but only 4mm maximum in turning because of its large support polygon. Since the workspace of the proposed overconstrained robotic leg is convex downwards, a down amplitude is generated in the stance phase, which is unwanted in most situations. With a 100mm stride length, the down amplitude of the forward trajectory is 3.4mm, which means that the fluctuation of CoG at least 3.4mm during locomotion. While the downward amplitude is 10mm for the lateral trajectory. The main reason for the extra fluctuation is the lack of the

robot body's altitude control. Another reason contributed is the extension of the foot ignored in the modeling. This reason also leads to a 20mm steering radius on turning, see Fig. 8(c).

B. Experiment verification with a Single Leg Module

Following the gait simulation, we also conducted an explorative verification of the omni-directional gait patterns of the robotic Bennett leg module. We programmed a python script on the PC to send position control commands to the motor driver (ODrive) via UART, and the motor driver communicated with the encoder via ABI interface for closed-loop control. The reference foot trajectories are given as a planar ellipse-like trajectory, a forward walking trajectory, and a lateral walking trajectory, recorded with the leg hanging in the air.

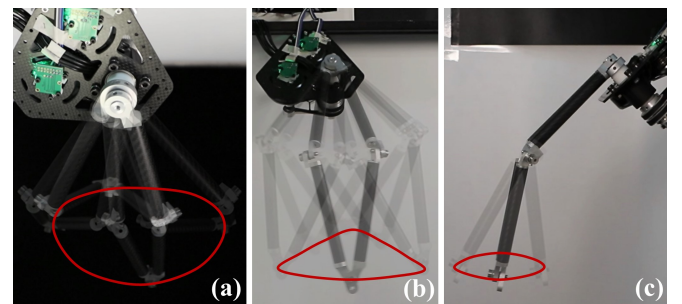


Fig. 9: The spatial trajectories of the Bennett leg in multiple viewpoints. (a) An ellipse-like trajectory tracking. (b) An forward walking trajectory tracking. (c) An lateral walking trajectory tracking.

The results are shown in Fig. 9, where an ellipse-like trajectory with a primary axis length of 260mm and a minor axis length of 150mm was used. The forward trajectory's stride length and ground clearance are set to 200mm and 50mm, while 150mm and 30mm in lateral trajectory. The robotic module with dual QDDs is well-capable of reproducing the planned trajectory in simulation to support a forward, sideways, and turning on the spot gait using only two actuators with an overconstrained Bennett leg.

V. DISCUSSION

A. Comparison of Leg Mechanisms with Dual Actuation

Although the proposed leg design with overconstrained linkages provides extra benefits in motion patterns on lateral walking and turning on the spot using only two actuators, it is necessary to compare it with other common dual actuated leg mechanisms kinematically. Table I shows the comparison of the Bennett leg with common two-link serial legs and planar five-bar legs. Since a remote placement of actuators closer to the robot body become a priority design to reduce leg inertia for enhanced agility, we selected Mini Cheetah [10] and Minitaur [5] as the reference for the leg parameters. The motion range of the overconstrained robotic leg is under the actual constraint, and the leg lengths of the three legs in full extend configuration are standardized as 0.3m.

TABLE I: Comparison of three leg mechanisms with dual outputs.

| Leg Mechanism | Two-bar Serial Leg [10] | Planar Five-bar Leg [5] | Overconstrained Bennett Leg |
|-------------------------------|-------------------------|-------------------------|-----------------------------|
| Cost of Agility | 1 | 1 | 0.8 |
| Workspace (m ²) | 0.141 | 0.126 | 0.206 |
| Force Transmission (Nm) | Joint 1 Joint 2 | 6.26 4.44 | 3.67 3.67 |
| Velocity Transmission (rad/s) | Joint 1 Joint 2 | 12.20 16.10 | 18.80 18.80 |
| | | | 10.27 |

The evaluation includes the cost of agility, workspace, force transmission capability, and velocity transmission capability. The serial leg has higher dexterity than the parallels to operate with different leg configurations. Nevertheless, we believe it is not necessary for robot ground mobility. The overconstrained Bennett leg has a 46.1% larger workspace at the reasonable cost of dexterity decrease. The ratio of degree-of-actuation (DoA) to the dimension of workspace is selected to evaluate the cost of agility. In this evaluation, the overconstrained robotic leg is only $\frac{2}{2.5} = 0.8$, while others are 1. This 20% advantage is contributed by the third coupled dimension of the workspace. We adopt the average actuator torque required to generate a 49N vertical foot force to investigate the force transmission capability and the average actuator speed required to generate a 2m/s foot velocity in forward direction to measure the velocity transmission capability. The calculation of these two capabilities is based on the whole workspace with the sampling points separated by 1mm. Thanks to actuators' parallel arrangement, the overconstrained Bennett leg has a lower torque requirement than the serial leg, with a 26.4% decrease. Without optimization, the overconstrained Bennett leg has the best performance of velocity transmission, which is 36.4% higher than the serial leg and 45.4% higher than the five-bar leg.

However, some limitations of the overconstrained robots need to be considered. Under specific configurations, the overconstrained robotic leg needs a larger volume for free rotation and more attention to a collision. Compared with the independently actuated legs, our design inevitably requires a longer swing trajectory for stride and may also require extra care on path planning. Nevertheless, this trade-off brings the reduction of DoA and the great advantage of omnidirectional ground mobility that exceeds existing robotic legs.

B. From Mechanism Intelligence to Biological Observation

To our best knowledge, the proposed overconstrained robotic leg is the first two-DoF leg capable of omnidirectional legged mobility including lateral walking and turning on the spot as shown in Fig. 8(a). The existed quadrupeds benefit highly dynamic from planar four-bar mechanisms [6], [7], [24] but suffer low-efficient steering without adding a third actuator [10]. The proposed design performs omni-directional locomotion by only modifying two kinematic parameters (α, σ) of the four-bar linkage. Moreover, the cost reduction and performance improvement brought by such mechanical intelligence also bring new ideas to the design of legged robots. Whether spatial mechanisms such as overconstrained mechanisms can be used in the

innovative design of high-performance robots required more in-depth research in the future.

By observing the lateral walking behavior from the quadruped with Bennett legs in Fig. 8(a) (see the attached video for more), we found an interesting resemblance with life-like gait patterns. While many quadruped robots draw design inspirations from mammals such as cheetah and dogs, the one shown in our design behaves like arthropods, or crustaceans such as crabs to be more precise. For example, the abduction of robotic leg leading to a broader robot width. Our simulation results show that our quadruped lateral walking stability with Bennett legs is better than that of forward walking. Such characteristics are very similar to the crabs both in morphology and gait, as shown in Figs. 10(a) and (b).

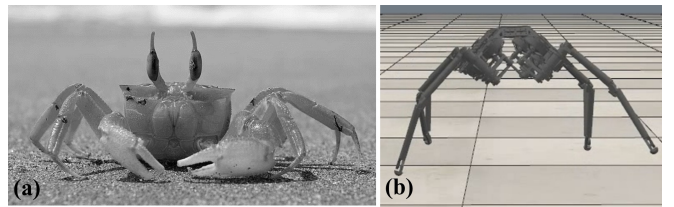


Fig. 10: The similar biological features between the crab and the overconstrained robots. (a) Image of a crab. (b) The overconstrained quadruped under lateral trotting.

C. Reconfigurable Design of Overconstrained Robots

It is useful to design a robot configuration for a specific task. Based on the method shown in section III, it is possible to design two types of joint modules with varying link parameters and assembly directions, including one with a low center of gravity (Low-CoG) and another with a high center of gravity (High-CoG), as shown in Fig. 11. On this basis, we can constructed the Low-CoG and High-CoG bipedal modules with a pair of robot joints. The Low-CoG robotic joint is suitable for multi-legged robots' crawling, while the High-CoG robotic joint is mainly used for upright walking. Hence, a new class of overconstrained robots can be reconstructed through a suitable combination of robotic joints or bipedal modules (as a leg or arm usage).

The resultant design can take various forms, including the quadruped, the lobster robot, the humanoid, and so on. The quadruped has four identical Low-CoG robotic joints connected by the carbon fiber plates and aluminum frames. The lobster robot was composed of four Low-CoG bipedal robot modules, one as the arm for manipulation and three as the leg for moving. The humanoid can be regarded as the combination of a Low-CoG bipedal module, a High-CoG bipedal module, and a body with electronics. Similar to the proposed Bennett modules, all robots in Fig. 11 shares the characteristics of a 33.3% reduction in the total number of actuators required using two actuators per module, instead of three, for 3D motion generation, resulting in a considerable reduction in weight and cost.

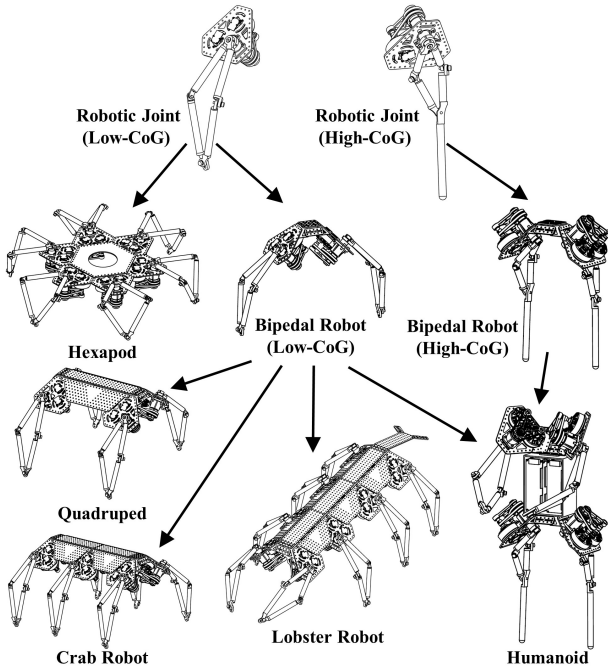


Fig. 11: Design reconfiguration of a class of overconstrained robots using the proposed Bennett limb with QDD.

VI. CONCLUSIONS AND FUTURE WORK

In this work, we consider a trade-off between locomotion agility and degree-of-actuation of robotic leg, and propose the novel design of an overconstrained robotic leg using the Bennett linkage. The robotic Bennett leg is driven by only two coaxially arranged quasi-direct drives, and capable of a coupled motion in a three-dimensional workspace. And the simulations indicated that the proposed design preserves the advantages of omni-directional quadrupedal locomotion, which is not the traditional planner legs with two DOFs can do. Furthermore, the Bennett leg provides the benefit of velocity transmission with 36.4% better than the two-bar serial leg, as well as the greater force transmission capability because of parallel actuation.

Future work includes the implementation of a full-size, overconstrained quadruped with agile locomotion and the exploration of additional control schemes to fully utilize its extreme mobility. Making a real-world robotic platform, we further intend to equip overconstrained quadruped with a thruster-based robotic limb, capable of multi-mode operations for unstructured exploration in the amphibian environment.

REFERENCES

- [1] U. Saranli, M. Buehler, and D. E. Koditschek, "Rhex: A simple and highly mobile hexapod robot," *The International Journal of Robotics Research*, vol. 20, no. 7, pp. 616–631, 2001.
- [2] S. Kim, J. E. Clark, and M. R. Cutkosky, "isprawl: Design and tuning for high-speed autonomous open-loop running," *The International Journal of Robotics Research*, vol. 25, no. 9, pp. 903–912, 2006.
- [3] G. C. Haynes, J. Pusey, R. Knopf, A. M. Johnson, and D. E. Koditschek, "Laboratory on legs: an architecture for adjustable morphology with legged robots," in *Unmanned Systems Technology XIV*, vol. 8387. International Society for Optics and Photonics, 2012, p. 83870W.
- [4] W. Bosworth, S. Kim, and N. Hogan, "The mit super mini cheetah: A small, low-cost quadrupedal robot for dynamic locomotion," in *2015 IEEE International Symposium on Safety, Security, and Rescue Robotics (SSRR)*. IEEE, 2015, pp. 1–8.
- [5] A. D. Gavin Kenneally and D. E. Koditschek, "Design principles for a family of direct-drive legged robots," *IEEE Robotics and Automation Letters*, vol. 1, no. 2, pp. 900–907, July 2016.
- [6] N. F. Nathan Kau, Aaron Schultz and P. Slade, "Stanford doggo: An open-source, quasi-direct-drive quadruped," in *International Conference on Robotics and Automation (ICRA)*, Montreal, Canada, May 2019, pp. 6309–6315.
- [7] S. Seok *et al.*, "Design principles for energy-efficient legged locomotion and implementation on the mit cheetah," *IEEE/ASME Trans. Mechatronics*, vol. 20, no. 3, pp. 1117–1129, June 2015.
- [8] M. Hutter, C. Gehring, D. Jud, A. Lauber, C. D. Bellicoso, V. Tsounis, J. Hwangbo, K. Bodie, P. Fankhauser, M. Bloesch, *et al.*, "Anymal—a highly mobile and dynamic quadrupedal robot," in *2016 IEEE/RSJ International Conference on Intelligent Robots and Systems (IROS)*. IEEE, 2016, pp. 38–44.
- [9] F. Grimminger, A. Meduri, M. Khaviv, J. Viereck, M. Wüthrich, M. Naveau, V. Berenz, S. Heim, F. Widmaier, T. Flayols, *et al.*, "An open torque-controlled modular robot architecture for legged locomotion research," *IEEE Robotics and Automation Letters*, vol. 5, no. 2, pp. 3650–3657, 2020.
- [10] B. G. Katz, "A low cost modular actuator for dynamic robots," Master's thesis, Massachusetts Institute of Technology, USA, 2018.
- [11] G. Bledt, M. J. Powell, B. Katz, J. Di Carlo, P. M. Wensing, and S. Kim, "Mit cheetah 3: Design and control of a robust, dynamic quadruped robot," in *2018 IEEE/RSJ International Conference on Intelligent Robots and Systems (IROS)*. IEEE, 2018, pp. 2245–2252.
- [12] K. Weinmeister, P. Eckert, H. Witte, and A.-J. Ijspeert, "Cheetah-cub-s: Steering of a quadruped robot using trunk motion," in *IEEE international symposium on safety, security, and rescue robotics (SSRR)*, West Lafayette, USA, Oct 2015, pp. 1–6.
- [13] S. Rezazadeh and J. W. Hurst, "Control of atrias in three dimensions: Walking as a forced-oscillation problem," *The International Journal of Robotics Research*, p. 0278364920916777, 2020.
- [14] C. D. Bellicoso, M. Bjelonic, L. Wellhausen, K. Holtmann, F. Günther, M. Tranzatto, P. Fankhauser, and M. Hutter, "Advances in real-world applications for legged robots," *Journal of Field Robotics*, vol. 35, no. 8, pp. 1311–1326, 2018.
- [15] S. Kalouche, "Design for 3d agility and virtual compliance using proprioceptive force control in dynamic legged robots," *MS dissertation*, 2016.
- [16] M. Russo, S. Herrero, O. Altuzarra, and M. Ceccarelli, "Kinematic analysis and multi-objective optimization of a 3-upr parallel mechanism for a robotic leg," *Mechanism and Machine Theory*, vol. 120, pp. 192–202, 2018.
- [17] S. Seok, A. Wang, D. Otten, and S. Kim, "Actuator design for high force proprioceptive control in fast legged locomotion," in *2012 IEEE/RSJ International Conference on Intelligent Robots and Systems*. IEEE, 2012, pp. 1970–1975.
- [18] G. T. Bennett, "A new mechanism," *Engineering*, vol. 76, pp. 777–778, 1903.
- [19] C. Song and Y. Chen, "A spatial 6r linkage derived from subtractive goldberg 5r linkages," *Mechanism and machine theory*, vol. 46, no. 8, pp. 1097–1106, 2011.
- [20] D. J. Blackman, J. V. Nicholson, C. Ordóñez, B. D. Miller, and J. E. Clark, "Gait development on minitaur, a direct drive quadrupedal robot," in *Unmanned Systems Technology XVIII*, vol. 9837. International Society for Optics and Photonics, 2016, p. 98370I.
- [21] R. M. Walter and D. R. Carrier, "Ground forces applied by galloping dogs," *Journal of Experimental Biology*, vol. 210, no. 2, pp. 208–216, 2007.
- [22] C. R. Carignan and K. R. Cleary, "Closed-loop force control for haptic simulation of virtual environments," 2000.
- [23] C. Song, H. Feng, Y. Chen, I. Chen, and R. Kang, "Reconfigurable mechanism generated from the network of bennett linkages," *Mechanism and Machine Theory*, vol. 88, pp. 49–62, 2015.
- [24] P. Arm, R. Zenkl, P. Barton, L. Beglinger, A. Dietsche, L. Ferrazzini, E. Hampp, J. Hinder, C. Huber, D. Schaufelberger, *et al.*, "Spacebok: A dynamic legged robot for space exploration," in *2019 International Conference on Robotics and Automation (ICRA)*. IEEE, 2019, pp. 6288–6294.